Journal of Pain Research

Dovepress
Taylor & Francis Group

Open Access Full Text Article

ORIGINAL RESEARCH

Activation of TLR4/CCL2 in Intact Neurons Drives Radicular Injury-Induced Global Nerve Trunk Hypersensitivity in Radiculopathy Preclinical Models

Si-Han Tong[1,2,*], Jian Zhou[1,2,*], Fang Ye[3,*], Peng Ding[1,2], Jia-Lun Mei[1,2], Peng Liao[4], Ya-Fei Lu[1,2], Yao Zong[5], Chu-An Gao[1,2], Sen-Yao Zhang[1,2], Jun-Jie Gao[1,2], De-Lin Liu[1,2], Yi-Gang Huang[1]

[1]Department of Orthopaedics, Shanghai Sixth People's Hospital Affiliated to Shanghai Jiao Tong University School of Medicine, Shanghai, 200233, People's Republic of China; [2]Institute of Microsurgery on Extremities, and Department of Orthopedic Surgery, Shanghai Sixth People's Hospital Affiliated to Shanghai Jiao Tong University School of Medicine, Shanghai, 200233, People's Republic of China; [3]Bone Marrow Transplantation Center, First Affiliated Hospital, and Liangzhu Laboratory, Zhejiang University School of Medicine, Hangzhou, 310000, People's Republic of China; [4]Department of Orthopaedics and Traumatology, Li Ka Shing Faculty of Medicine, The University of Hong Kong, Hong Kong SAR, People's Republic of China; [5]Centre for Orthopaedic Research, Medical School, The University of Western Australia, Nedlands, Perth, Western Australia, 6009, Australia

*These authors contributed equally to this work

Correspondence: Yi-Gang Huang; De-Lin Liu, Email yiganghuang@sjtu.edu.cn; 7250013413@shsmu.edu.cn

Introduction: The distribution of pain in painful radiculopathy extends beyond the region innervated by the injured nerve. This phenomenon may arise due to the interaction between damaged nerve fibers and intact ones within the same nerve trunk. However, the underlying mechanisms remain unclear.

Methods: An L5 spinal nerve compression rat model was established. RNA sequencing (RNA-seq) was performed to identify altered signaling pathways in the L4 dorsal root ganglia (DRG). Nociceptive behaviors were evaluated by von Frey testing and gait analysis. Immunofluorescence stainings were employed to analyze protein expression levels. Primary DRG neurons were cultured for in vitro validation of key molecular pathways.

Results: We observed that degenerated L5 nerve fibers released damage-associated molecular patterns (DAMPs), which may activate Toll-like receptor 4 (TLR4) signaling in intact L4 nerve fibers mingling in the sciatic nerve. This activation led to increased expression of C-C chemokine ligand 2 (CCL2), which induced macrophage infiltration and upregulation of ion channels in the L4 DRG. Administration of TAK-242, a TLR4 antagonist, reduced the neuronal expression of CCL2 in the L4 DRG and attenuated pain-like behavior in nerve-compression rats.

Conclusion: Our findings demonstrate that L5 spinal nerve lesions activate TLR4/CCL2 signaling in adjacent uninjured L4 neurons within the sciatic nerve, leading to a global nerve trunk hypersensitivity. Targeting the TLR4/CCL2 pathway may provide a novel therapeutic strategy for the management of radiculopathy.

Keywords: painful radiculopathy, nerve trunk hypersensitivity, uninjured neuron, CCL2, TLR4

Introduction

Painful radiculopathy, the most common neuropathic pain condition, is caused by damage to the spinal nerve roots, bringing chronic disability and financial burden to patients.[1,2] Although abnormal activation of injured nerve fibers has been largely studied,[3] pain sometimes does not correspond to the injured segment-innervated area.[4] In cervical radiculopathy patients, lesion of the C8 nerve, which mainly contributes to the median nerve motor response, also results in C6/C7 nerve-innervated paresthesia.[5] Meanwhile, in a rat model of L5 spinal nerve ligation (SNL), L4 neurons were activated, and a L5 dorsal rhizotomy before surgery did not prevent thermal hyperalgesia.[6,7] Additionally, dorsal

Received: 8 November 2024
Accepted: 24 June 2025
Published: 4 August 2025

Graphical Abstract

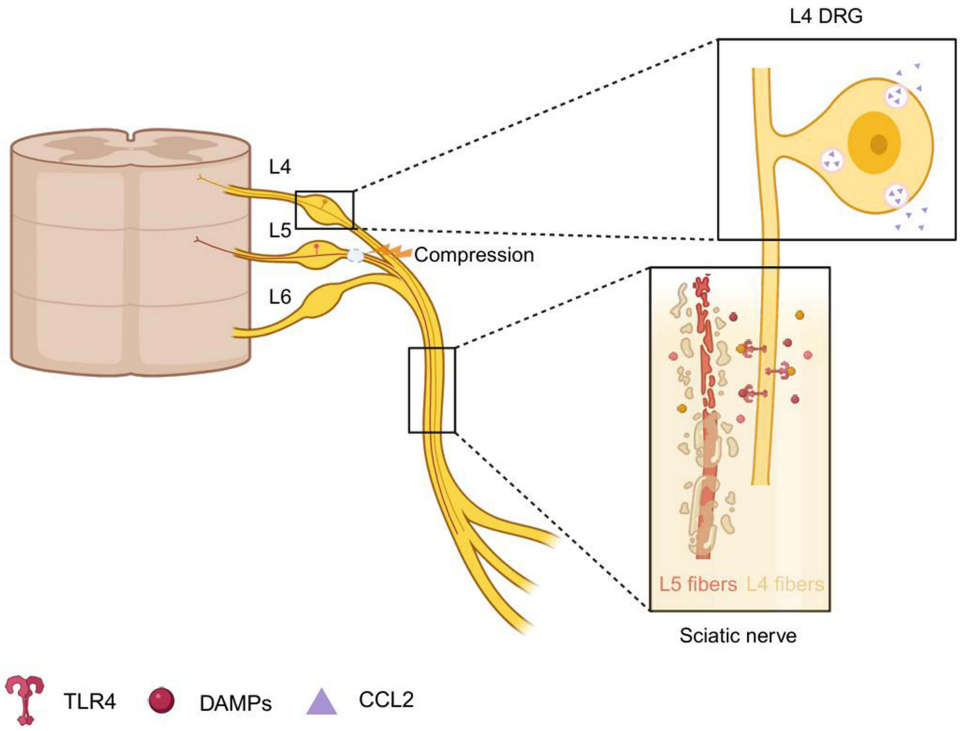

root ganglion stimulation is an analgesic neuromodulation approach, while stimulation of the ganglion at multiple levels is usually more efficient in decreasing hypersensitivity than the single level.[8] These studies suggest that the adjacent uninjured DRG segment might also participate in the development of pain.

In some classical L5 spinal nerve injury models, neighboring L4 fibers showed spontaneous firing and lower electrical threshold,[7,9,10] accompanied by upregulation of pain-promoting substances, including brain-derived neurotrophic factor (BDNF), calcitonin gene-related peptide (CGRP), Cav3.2, and TRPV1.[6,7,11] Some mechanisms have been proposed to explain these changes in L4 DRG. One of them is that the ectopic activity arising from injured afferents sensitizes spinal dorsal horn neurons, and the uninjured afferents connecting to sensitized spinal neurons are proposed to convey extra stimuli.[12] The other is that, since L5 nerve fibers converge with L4 nerve fibers in the sciatic nerve trunk,[13] the increase of cytokines and growth factors induced by L5 Wallerian degeneration influences L4 neurons through their commingled nerve fibers. We refer to this as radicular injury-induced global nerve trunk hypersensitivity. For instance, nerve growth factor (NGF) could act on nearby sensory fibers along the course of the nerve and induce kinase activation in the adjacent intact L4 DRG neurons.[6] High mobility group box 1 (HMGB1), generated by macrophages in the sciatic nerve, upregulates calcium channel 3.2 in L4 DRG after L5 spinal nerve cutting.[11] Furthermore, some inflammatory mediators or acidic PH in a degenerative environment could activate TRPV1 along the axons, resulting in spontaneous firing.[9]

CCL2, also named monocyte chemoattractant protein-1, is a classical chemokine that plays a pivotal role in the development of pain.[14,15] It could not only increase the excitability of neurons directly but also recruit immune cells.[16–18] In a model of osteoarthritis, expression of CCL2 was induced by toll-like receptor 4 (TLR4) activation in sensory neurons. After nerve injury, degenerative nerves that contain damaged axons, activated Schwann cells, and immune cells can release damage-associated molecular patterns (DAMPs), which were reported as agonists for TLR4.[19] However, whether the TLR4/CCL2 pathway participates in the hypersensitivity of adjacent neurons in painful radiculopathy remains unclear. In this article, we performed a rat model of L5 spinal nerve compression to mimic painful radiculopathy

and showed that the degenerated L5 axons can activate TLR4 in L4 neurons and induce CCL2 expression, promoting the hypersensitivity of the global nerve trunk and pain development.

Materials and Methods

Animals and L5 Spinal Nerve Compression Model

Adult male Sprague-Dawley rats (6 weeks) were housed at room temperature during a 12-hour light-dark cycle and had free access to food and water. To establish the L5 spinal nerve compression model, the limbs of rats were fixed in a prone position after peritoneal anesthesia with pentobarbital sodium. The skin of rats was made a 3cm-long incision between the spine and the right crista iliaca. The muscle was separated in the open direction and then we used a vessel clamp to carefully remove the L6 transverse process to expose the L5 spinal nerve root. In the L5 compression group, the L5 nerve was wrapped with a cannula with an external diameter of 1mm and an internal diameter of 0.5mm. 6–0 sutures were passed through and knotted over the cannula to ensure no shedding. In the sham group, the cannula was only embedded next to the L5 nerve. After surgery, the incision was washed with a large amount of normal saline and the muscle and skin layers were closed by 3–0 sutures.

All animal experiments were approved by the Animal Care and Use Committee of Shanghai Sixth People's Hospital. The operation was performed after anesthesia with pentobarbital sodium, and all efforts were made to minimize suffering.

TAK-242 Treatment in vivo

For the in vivo experiment of TLR4 inhibitor treatment, TAK-242 (MCE, Cat. HY-11109) was dissolved in dimethyl sulfoxide (DMSO), and the process was performed following a previously reported method.[20] In the treatment group, TAK242 (3mg/kg) was intraperitoneally (i.p.) injected into the rats 30 minutes before L5 nerve compression, while rats in the untreated group were injected with 200μL of DMSO.

Von Frey Test

Pain behavior in rats was examined using the electronic von Frey test on the plantar surface of the right hind paw. An electronic von Frey esthesiometer (BIO-EVF4; Bioseb, France) was used for the quantitative measurement of the mechanical hind paw withdrawal threshold (PWT). A pogo pin was used in the experiment. The chip was slowly applied to the center of the plantar area of the hind paw and pressed gradually; the pressure was automatically measured when the rat spontaneously lifted its hind paw. Ten trials were performed per rat, and the PWT was obtained by removing the minimum and maximum values and calculating the average of the remaining eight values. The stimulation interval was at least 1 minute for each rat. Fifteen rats were allocated to the von Frey test.

Hotplate Test

The hotplate test was performed by placing the animals on a hotplate system (35100; Ugo Basile, Italy), with a surface temperature of 52°C. The nociceptive threshold was quantified as the latency (in seconds) to licking, retraction of the hind paw, or jumping after placement of the rat on the hotplate. A 30-s cut off was used to avoid tissue damage. Fifteen rats were allocated to the hotplate test.

Gait Analysis

Rats' gait was analyzed by CatWalk automated gait analysis system (Noldus Information Technology). The system has a glass plate with a green LED light and a high-speed video camera to capture their footprint. Before the formal experiment, the rats were placed on the plate to acclimate the environment. Several compliant runs without stopping, changing direction, and turning around were analyzed with CatWalk Software. Data were generated by VisuGait Software after each footprint was checked manually. Twenty-two rats were allocated to gait analysis.

RNA Isolation and Real-Time Quantitative PCR

For isolating RNA from cells, an RNA purification kit for cells (EZBioscience, Cat. B0004DP) was utilized according to the manufacturer's protocol. For isolating RNA from tissue, DRG was crushed in a tissue grinder machine (Servicebio). RNA was isolated using the RNA purification kit (EZbioscience, Cat. EZB-RN001-plus) according to the manufacturer's protocol. An additional DNase1 digestion step was performed to ensure that the samples were not contaminated with genomic DNA. RNA concentration was assessed with Nanodrop spectrophotometers (Thermo Fisher Scientific, QuantStudio™ 7 Flex Real-Time PCR System, QuantStudio Real-Time PCR 1.3).

For reverse transcription, 1000 ng RNA was reverse transcribed using 4×Reverse Transcription Master Mix (EZbioscience, Cat. EZB-RT2GQ). qPCR was performed using 2×SYBR Green Color qPCR Mix (EZbioscience, Cat. A0001-R1) following the manufacturer's recommendation. Samples were tested on a Quant StudioTM 7 Flex Real-Time PCR System (Thermo Fisher Scientific). The results were calculated using the ΔΔCT method and are presented as the x-fold increase relative to GAPDH mRNA levels. Primers were synthesized by Tsingke company and are listed in (Supplementary Table 1). Thirty-two rats were allocated to the qPCR experiment.

Histological Section and Luxol Fast Blue (LFB) Staining

L4, L5 spinal nerve and sciatic nerve were collected from rats and fixed in the 4% PFA for 24 hours. 4μm-thick paraffin-embedded sections were obtained for further staining. For LFB staining, sections were deparaffinized and rehydrated sequentially with xylene and alcohol, followed by incubation with LFB solution (Servicebio, Cat. G1030) at 60 °C for 1h. Subsequently, slices were washed with dd H2O to terminate differentiation, repeated washing until the myelin sheath was blue and the background was almost colorless. Then, put the section into a hematoxylin solution for counterstaining. Finally, the section was dehydrated by ethanol and sealed by neutral gum. Imaging was performed on a microscope (Nikon, Eclipse C1, Japan). Four rats were allocated to LFB staining.

Hematoxylin-Eosin (HE) Staining

The sections were deparaffinized in xylene and rehydrated through 100, 90, 80, and 70% ethanol. Then, we rinsed the sections in PBS for 5 min. After staining, pathological sections were examined using a microscope (Nikon, Eclipse C1, Japan). Two rats were allocated to HE staining.

Bulk RNA-Seq

RNA Extraction

The limbs of rats were fixed in a prone position after peritoneal anesthesia with pentobarbital sodium. The L4, L5 DRGs and sciatic nerve were carefully dissected and collected. The total RNA was extracted from tissue samples using the "Guanidine isothiocyanate-phenol-chloroform extraction" method. The concentration and purity of RNA were detected by Nanodrop 2000 before reverse transcription.

Library Preparation for Transcriptome Sequencing

A total amount of 1 μg RNA per sample was used as input material for the RNA sample preparations. Sequencing libraries were generated using NEBNext® Ultra™ RNA Library Prep Kit for Illumina® (NEB, USA) following manufacturer's recommendations and index codes were added to attribute sequences to each sample. The library fragments were purified with AMPure XP system (Beckman Coulter, Beverly, USA) to select cDNA fragments of preferentially 250~300 bp in length. Then, 3 μL USER Enzyme (NEB, USA) was used with size-selected, adaptor-ligated cDNA at 37°C for 15 min followed by 5 min at 95°C before PCR. Then, PCR was performed with Phusion High-Fidelity DNA polymerase, Universal PCR primers and Index (X) Primer. At last, PCR products were purified (AMPure XP system) and library quality was assessed on the Agilent Bioanalyzer 2100 system.

Quality Control

Raw data (raw reads) of fastq format were first processed through in-house perl scripts. In this step, clean data (clean reads) were obtained by removing reads containing adapter, reads containing ploy-N and low-quality reads from raw data. At the same time, Q20, Q30 and GC content of the clean data were calculated. All the downstream analyses were based on clean data with high quality.

Analysis of RNA-Seq Data

After quality control, raw sequencing reads were aligned to the mouse reference genome (GRCm38) using STAR (version 2.7) with the default settings.[21] We used featuresCounts (version 1.6.0) with the following parameters: "featureCounts -T 40 -p -t exon -g" to generate gene-level read counts.[22] Differential gene expression levels were calculated using DEseq2 (version 1.28.1) and gene annotations were obtained from Ensembl.[23] The gene expression correlations of different samples were evaluated using PCA analysis and visualized in heatmap and scatter plot with default settings.

Gene Ontology (GO), Kyoto Encyclopedia of Genes and Genomes (KEGG) Pathways and Gene Set Enrichment Analysis (GSEA)

For gene function analysis Gene ontology (GO), Kyoto Encyclopedia of Genes and Genomes (KEGG) pathways analysis are performed using top differentially expressed genes (top 300–500, padj<0.05, log2FoldChange>1). GO enrichment (biological process and cellular composition) and KEGG pathway enrichment are calculated using R package clusterProfiler with default settings (pvalueCutoff = 0.01, qvalueCutoff = 0.05 for GO enrichment,[24] pvalueCutoff = 0.01, pAdjustMethod = "BH", minGSSize = 10, maxGSSize = 500 for KEGG pathway enrichment). GSEA enrichment of all differentially expressed genes in each group is calculated using R package fgsea.[25] The data were deposited into the GEO repository (GSE246156). Six rats were allocated to bulk RNA-seq.

Flow Cytometry

After anesthesia, the rats were sacrificed by cervical dislocation. Next, L4 DRGs were carefully dissected and collected. The tissues were cut into small pieces by scissors. The tissues were soaked in papain solution (20U/mL) (Shanghai Yuanye Biological Technology Co., Ltd.) at 37°C for 30 minutes and the solution was filtered through a 70 μm cell strainer into a new 1.5 mL Eppendorf tube. The Eppendorf tubes were centrifuged for 5 minutes at 4°C, 5000 rpm. The supernatant was removed and the cell precipitate was suspended in 1mL of staining buffer (PBS, MeilunBio®, #MA0015-1; 1% fetal bovine serum, Gibco, #10100147). Then the cells were mixed with an antibody mixture (PE anti-rat CD45, Biolegend Antibody, Cat #202207; FITC Anti-rat CD68, Invitrogen, WA3171647) on ice away from light for 30 minutes. The cells were washed with 1 mL of staining buffer and centrifuged for 5 minutes at 4°C, 5000 rpm. The supernatant was aspirated and the cells were suspended in 300 μL staining buffer. Samples were analyzed using cytometer CytoFlex (Beckman Coulter) and FlowJo software version 10.4. Six rats were allocated to flow cytometry.

Primary Culture of Rat DRG Neurons and Treatment

DRG neurons were separated and maintained in vitro as previously reported.[26] In detail, DRG neurons from 4w Sprague-Dawley rats were dissociated with 0.25% Trypsin-EDTA (Gibco) and 0.1% collagenase II (Fushenbio) for 40 min, and then the individual DRG neurons were planted in DMEM medium (Gibco) with 10% FBS (Gibco) for 6 hours. Next, the medium was replaced with Neurobasal complete medium (Gibco) supplemented with 2% B27 (Gibco), 200 mM L-glutamine, and 1% Penicillin-Streptomycin (Gibco) to maintain cell growth. The neurons were maintained in a cell incubator (Thermo) at 37°C with 5% CO_2 and can be used for further experiments after 4 days. Twenty-four hours stimulation with 1ug/mL lipopolysaccharide (LPS) (MCE, Cat. HY-D1056) was performed. Then, cells and supernatant were collected for qPCR and enzyme-linked immuno sorbent assay (ELISA) respectively. Eleven rats were allocated to the primary culture of DRG neurons.

Immunofluorescence Staining and Confocal Imaging

For DRG immunofluorescence staining, after perfusing the heart with 50mL normal saline and 4% PFA, L4 DRGs were collected by cutting off the nerve trunk under a microscope. The collected DRGs were fixed in 4% PFA at 4 °C for an additional 12 hours and dehydrated in 30% sucrose for 24 hours. Then the DRGs were embedded in an O.C.T. compound (Sakura Finetek Cat. 4583) for 10 μm coronal sections with a cryostat microtome (Leica). After washing the O.C.T. compound with PBS, DRGs were permeabilized with 0.1% Triton X-100 for 10 minutes. Blockage of DRG was next performed with 3% bovine serum albumin (BSA) (SigmaAldrich Cat. A7030)/PBS for 1 hour. The primary anti-b3-tubulin antibody (1:200, Proteintech Group, Cat. 66375-1-lg), anti-3PGDH antibody (1:200, Santa Cruz, Cat. Sc-390610) and anti-CCL2 antibody (1:200, Affinity, Cat. DF7577) were incubated for 24 hours at 4 °C. After washing with PBS for 3 times, DRG were incubated with donkey anti-mouse IgG (H + L) cross-adsorbed secondary antibody Alexa Fluor 488 (1:200, Thermo Fisher Scientific, Cat. A21202) mixed with donkey anti-rabbit IgG (H + L) cross-adsorbed secondary antibody Alexa Fluor 568 (1:200, Thermo Fisher Scientific, Cat. A11057) for 2 hours at room temperature. After washing with PBS for 3 times, DRG samples were counterstained with DAPI for 15 minutes at room temperature. Next, sections were covered with coverslips after dropping the sealed neutral gum. Confocal images were instantly acquired on Olympus FV3000, Olympus SpinSR, or Zeiss 710 confocal microscope. Sixteen rats were allocated to DRG immunofluorescence staining.

For immunofluorescence staining of cell samples, cells were fixed with 4% PFA for 15 minutes followed by 20 minutes of permeabilization with 0.1% Triton X-100. Next, cells were washed with PBS for 3 times and then blocked with 3% BSA/PBS for 1 hour. Next, primary DRG cells were stained with the primary anti-b3-tubulin antibody (1:200, Proteintech Group, Cat. 66375-1-lg) for 24 hours at 4 °C. After washing with PBS 3 times, cells were incubated with donkey anti-mouse IgG (H + L) cross-adsorbed secondary antibody Alexa Fluor 488 (1:200, Thermo Fisher Scientific, Cat. A21202) for 2 hours at room temperature followed by 15 min incubation of DAPI. Next, 10 μL of the fluoromount was dipped on the microscope slide, and the glass coverslip was flipped on its top. The immunofluorescence was examined using a Leica SP8 confocal microscope. Three rats were allocated to cell immunofluorescence staining.

ELISA

Primary DRG neurons were treated with 1ug/mL LPS for 24 hours; then, the supernatants were centrifuged at 2000 g for 20 min and collected for analysis. In addition, the media from untreated were collected as the control. Commercial CCL2 ELISA kits (Elabscience, China) were used to detect the content of CCL2 in each group. Four rats were allocated to ELISA.

Statistical Analysis

Data are presented as the mean ± standard error of the mean (SEM) except were stated otherwise. Graphs and statistics were analyzed by GraphPad Prism (version 9.1.1). Detailed data processing, sample size and statistical methods for each result were shown in the corresponding figure legends. A two tailed Student's *t*-test was used for mean comparisons between the two groups. $p < 0.05$ was considered statistically significant.

Results

The Rat L5 Spinal Nerve Compression Model Showed Pain-Like Behavior

Painful radiculopathy is often caused by herniated disks, spinal column degeneration, trauma, and neoplastic disease,[3] resulting in physical compression of the spinal nerve root. Hence, we established a spinal nerve compression model. Summarily, we bit away the right L6 transverse process with a vascular clamp and wrapped around the right L5 spinal nerve using a cannula with an inner diameter of 0.5 mm, which is half of the nerve diameter (Figure 1A). After removing the transverse process, the cannula was buried next to the L5 nerve root in the sham-operated group. To certify that our surgery did not induce L4 axonal degeneration, we performed LFB and hematoxylin staining of the distal part of the compression site. The results showed that the L5 spinal nerve trunk was degenerating with cell expansion, and the L4 spinal nerve trunk was almost intact in the group of L5 compression (Figure 1B). Next, we evaluated the pain-like

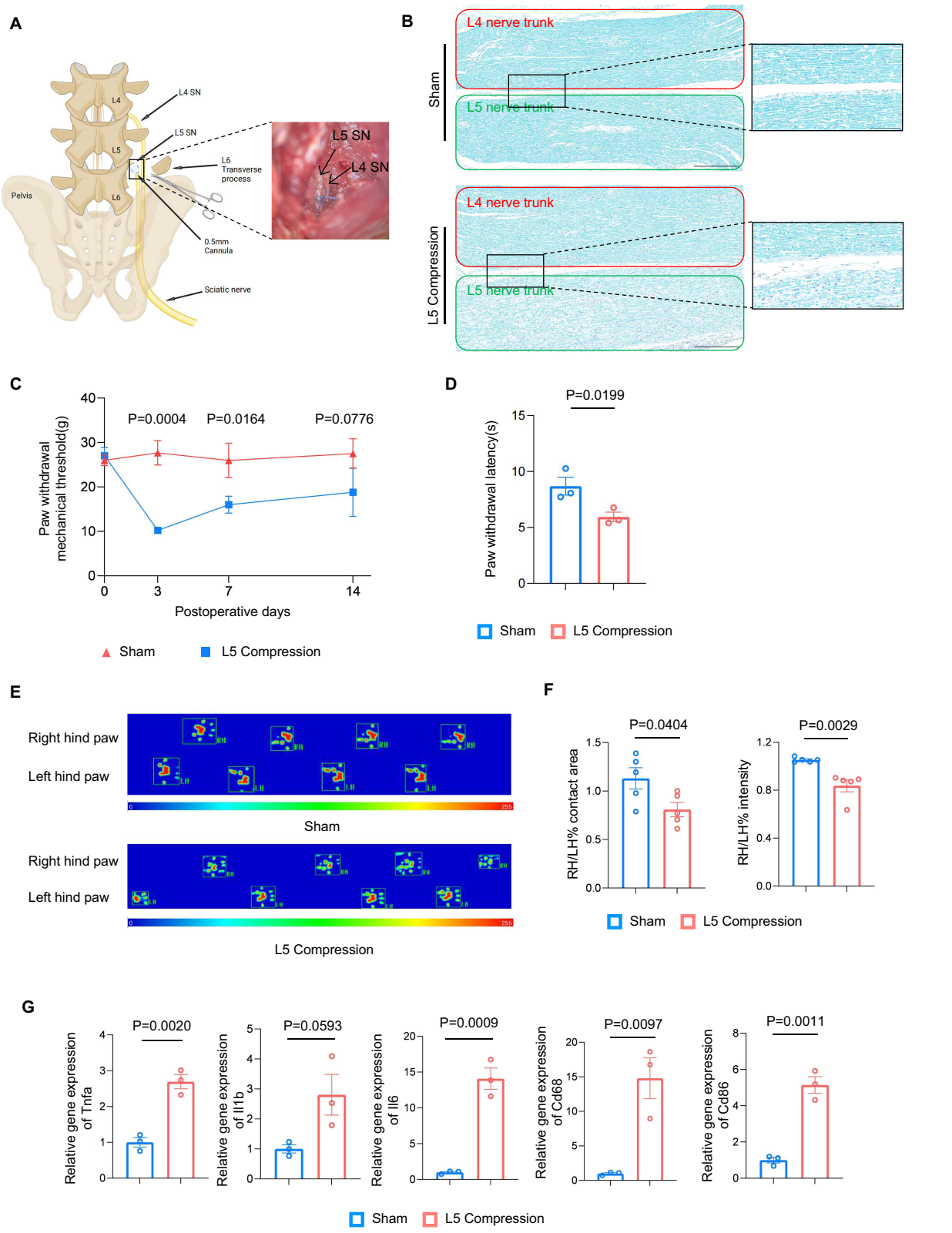

Figure 1 Establishment of rat L5 spinal nerve compression model. (**A**) Diagram and photo of L5 spinal nerve compression surgery. The L6 transverse process was bit away and the L5 spinal nerve was wrapped with a 0.5mm cannula. (**B**) FLB and hematoxylin staining of L4 and L5 nerve trunk at the distal end of compression position. Scale bar, 300um; insert, 100um. (**C**) Time-dependent changes in PWT after L5 compression surgery (Day 0, 3, 7, 14) (n=3). (**D**) PWL decreased in L5 compression group compared with sham group (n=3). (**E**) Representative images of gait analysis on POD3. (**F**) Contact area and intensity of the right hind paw compared to the left hind paw (n=5). (**G**) Quantitive real-time PCR revealed a significant increase in inflammation-related gene (*Tnf-a, Il-1b, Il-6, Cd68, Cd86*) expression in rat L5 DRG on POD3 (n=3).

https://doi.org/10.2147/JPR.S499997

behavior between our surgical and sham groups. The electrical von Frey test showed that the rats in the surgical group developed mechanical hypersensitivity on both POD3, 7 and 14, especially on POD3, which is similar to the acute phase of clinical radiculopathy (Figure 1C).[27] The hotplate test revealed a decreased paw withdrawal latency (PWL) in the L5 compression group (Figure 1D). Meanwhile, gait analysis revealed that the percentage of contact area and intensity of right hind paw versus left hind paw presented a significant disparity at 3 days after surgery relative to sham group (Figure 1E and F). We further compared gait patterns in rats subjected to L5 spinal nerve compression and traditional L5 spinal nerve ligation (SNL). The results demonstrated that our surgery significantly reduced motor function impairment in rats (Figure S1). In addition, the mRNA level of inflammatory factors such as *Tnf-a, Il-1b, Il-6, Cd68*, and *Cd86* was significantly elevated in L5 DRG (Figure 1G). The evidence above indicated that we successfully established the L5 nerve compression model and kept the movement function of the hind paw for evaluating behavioral changes in rats.

Upregulation of CCL2 in L4 Neurons After L5 Spinal Nerve Compression

After L5 spinal nerve injury, L4 neurons showed abnormal activation, such as spontaneous firing or lower electrical threshold.[7,9,10] To explore the underlying molecular mechanism, we performed L4 DRG bulk RNA-seq on POD3. The results indicated that differentially expressed genes were highly enriched in myeloid leukocyte activation, leukocyte migration, positive regulation of cytokine production, and leukocyte mediated immunity categories (Figure 2A). Meanwhile, KEGG enrichment analysis highlighted chemokine signal pathway, and leukocyte transendothelial migration signaling pathway (Figure 2B). These results showed that L5 spinal compression can induce inflammatory changes and chemokine-related responses in L4 DRG. Consistently, qPCR validation revealed that the mRNA level of *Ccl2*, which serves as an essential pain-related chemokine,[14] was significantly upregulated in L4 DRG on both POD3 and POD7 (Figure 2C). As CCL2 has been reported to induce the infiltration of macrophages,[18] increase sodium ion channels and activate transient receptor potential vanilloid 1 (TRPV1) or transient receptor potential A1 (TRPA1) channels,[28] we used flow cytometry and qPCR to verify CCL2 function. Our flow cytometry analysis of L4 DRG showed an increase in the number of $CD68^+$ labeled macrophages on POD3 (Figure 2D). Additionally, a transcriptional upregulation of *Nav1.7, Nav1.8* and *TRPV1* was found in L4 DRG on POD7 (Figure 2E), although we could not rule out the possibility that other inflammatory cytokines might also play a role in increase of ion channels. Next, to further clarify the cell types that express CCL2, we performed immunofluorescence and labeled DRG neurons with b3-tubulin. Immunofluorescence staining and confocal imaging revealed that CCL2 is mainly expressed in small and medium diameter neurons (<50um) (Figure 2F) but not satellite glial cells (Figure S2).[29] Furthermore, the L5 compression group showed higher fluorescence intensity of CCL2 protein versus the sham group (Figure 2G).

DAMPs Were Significantly Increased in the Sciatic Nerve

Rat L4 and L5 spinal nerves emerge from the corresponding intervertebral foramina and then travel down, converging to form the sciatic nerve.[13] After L5 nerve injury, the intact fibers that derived from L4 root are exposed to an acute Wallerian degeneration environment in the L4/L5-comingled sciatic nerve trunk. Products from damaged axons, dedifferentiated Schwann cells, and infiltrated inflammatory cells alter the function of L4 fibers.[7,30] To investigate underlying factors that influence these intact neurons, we performed RNA sequencing of the sciatic nerve on POD3. GO enrichment of sciatic nerve in the surgery group highlighted chromosome segregation, DNA replication, and cell division items, indicating the occurrence of injury and repair responses in the acute post-surgery phase (Figure 3A). Moreover, the LFB and HE staining also showed the characteristic of axonal degeneration and inflammation in the sciatic nerve (Figure 3B). Studies have demonstrated that DAMPs in the joints of osteoarthritis patients can induce CCL2 expression in sensory neurons, resulting in mechanical allodynia.[31] Consistent with this, the gene heatmap of the POD3 sciatic nerve revealed a significant upregulation of DAMPs relative to the sham group, including heat shock proteins (HSPs), IL-1a (interleukin-1a), a2-macroglobulin (A2M), and high mobility group box 1 (HMGB1) (Figure 3C). Additionally, an increase of two DAMPs, *Il1a* and *A2m*, which were proven to be the candidates to induce expression of CCL2 in neurons,[31] was further detected by qPCR (Figure 3D). These results suggested that the sciatic nerve was degenerating, accompanied by increased DAMPs, which may play a role in inducing the expression of CCL2 in adjacent neurons.

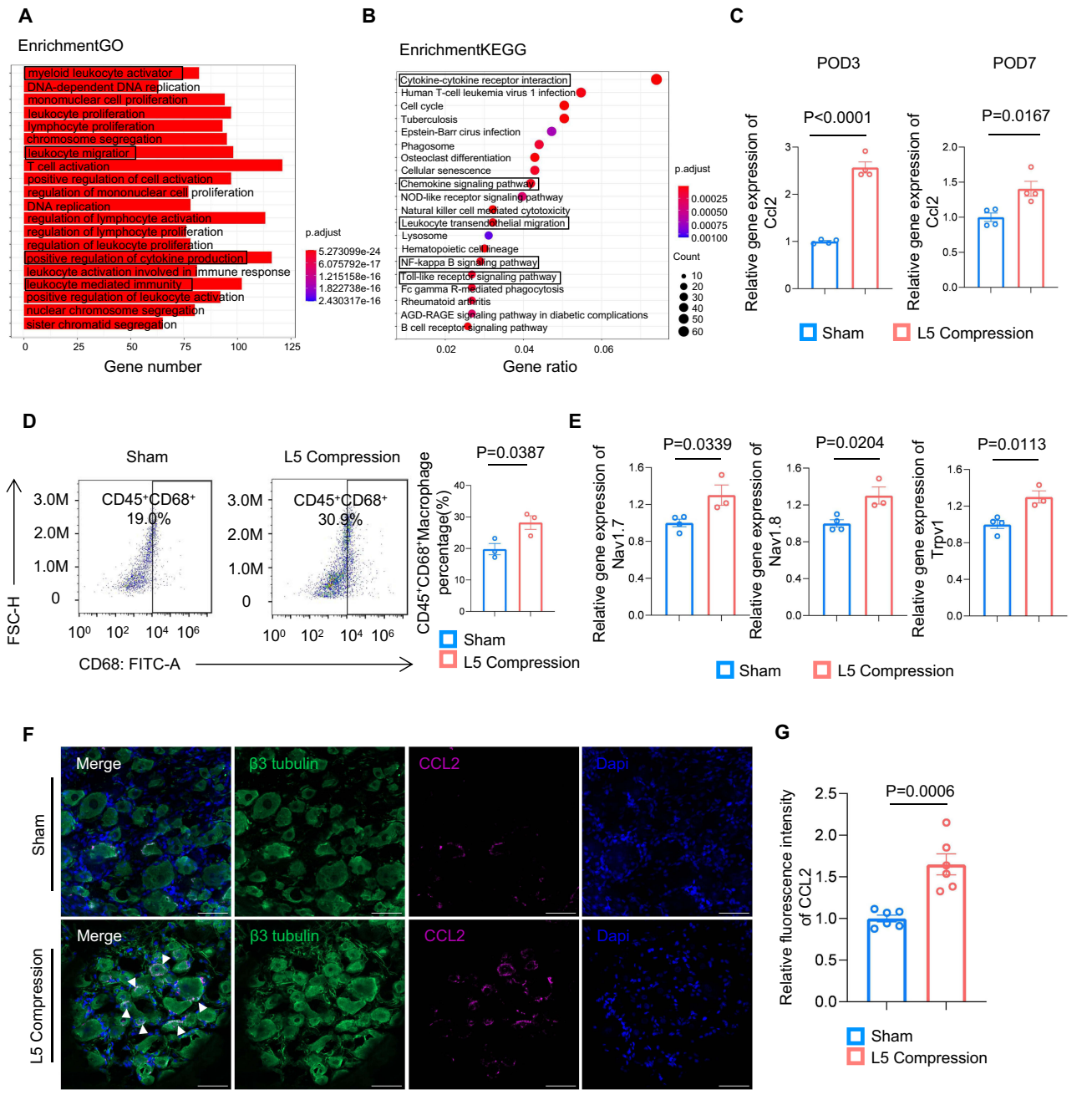

Figure 2 Upregulation of CCL2 in L4 neurons after L5 spinal nerve compression. (**A**) Paired enriched GO function items in the biological process of L4 DRG on POD3. (**B**) Paired KEGG pathway of L4 DRG on POD3. (**C**) Relative gene expression of *Ccl2* upregulated at both POD3 (n=4) and POD7 (n=4). (**D**) FACS revealed an increase in $CD45^{+}CD68^{+}$ labeled cells on POD3 (n=3). (**E**) Relative gene expression of *Nav1.7, Nav1.8* and *Trpv1* upregulated at POD7 (Sham group n=4, L5 Compression group n=3). (**F**) Representative images of b3 tubulin (green) and CCL2 (pinkish red) in rat L4 DRG on POD3. White arrows showed co-localization of CCL2 and b3 tubulin. Scale bar, 50um. (**G**) Relative fluorescence intensity of CCL2 of sham group versus L5 nerve compression group (6 dots from 3 rats in each group).

TAK-242 Injection Reduced CCL2 Expression in L4 DRG

Since KEGG enrichment analysis highlighted chemokine, NF-kappa B, and Toll-like receptor signaling pathway in L4 DRG after L5 compression (Figure 2B), and previous research reported that DAMPs were able to activate TLR4 and upregulate the expression of CCL2 in DRG neurons,[31,32] we wonder if TLR4 activation could induce CCL2 elevation in L4 DRG after L5 compression. Gene heatmap of L4 DRG showed that TLR4 pathway-related genes, such as *Myd88, Irak1, Irak4*, and *Nfkb1*, were significantly increased after L5 compression (Figure 4A). Meanwhile, qPCR revealed that gene expression of *Tlr4* was upregulated in L4 DRG (Figure 4B). To further elucidate the function of TLR4, we

https://doi.org/10.2147/JPR.S499997

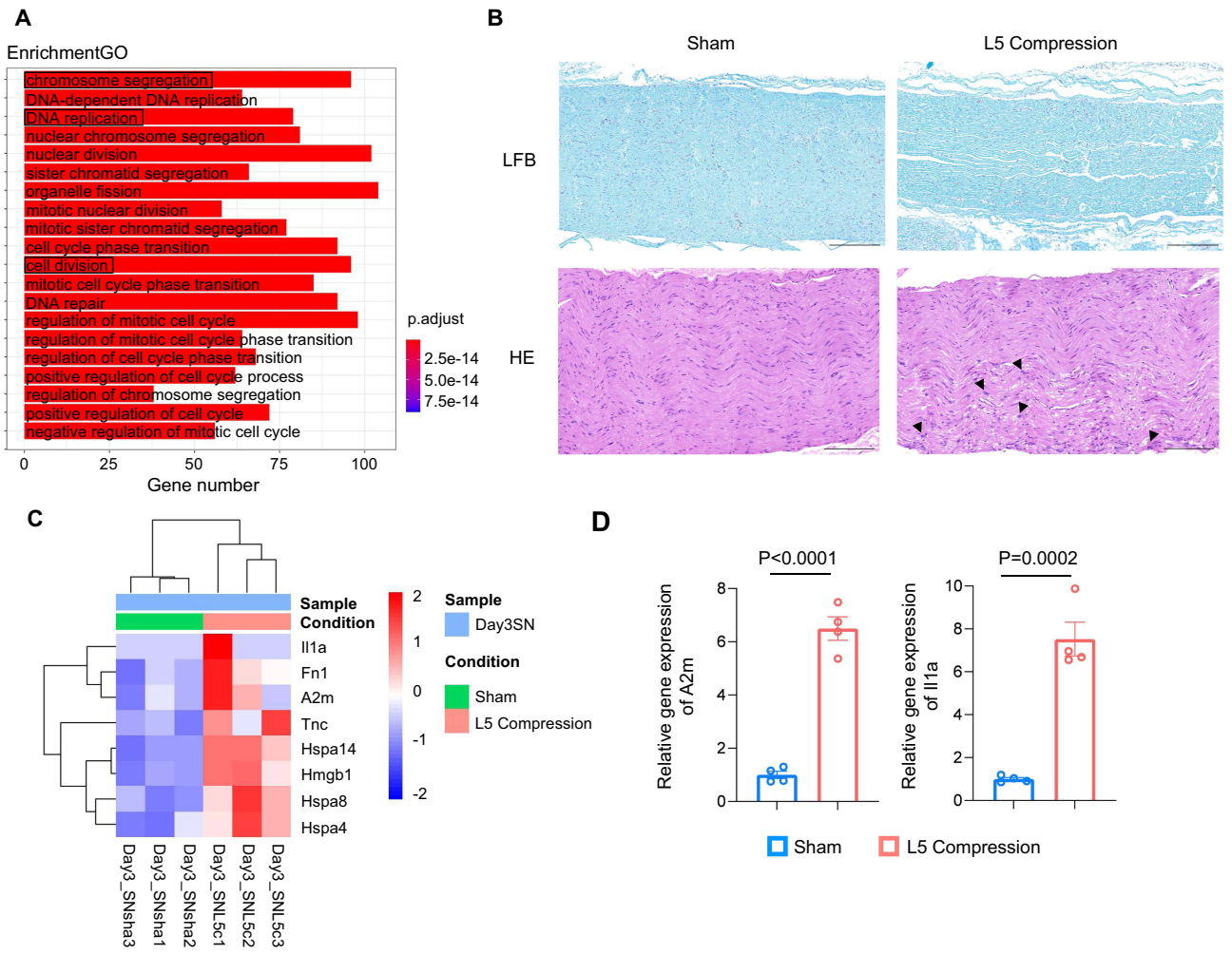

Figure 3 Upregulation of DAMPs in sciatic nerve. (**A**) GO enrichment analysis indicated degeneration occurred in the sciatic nerve. (**B**) LFB and HE staining of the sciatic nerve on POD3. Black arrows showed inflammatory cells. Scale bar, 300um. (**C**) Gene heatmap of DAMPs in the sciatic nerve on POD3. (**D**) Relative gene expression of *A2m* and *Il1a* significantly increased (n=4).

performed an i.p. injection with the TLR4 antagonist, TAK-242, 30 minutes before our surgery.[20] Consistent with our hypothesis, after 3 days, qPCR and immunofluorescence results showed that CCL2 expression was reduced at both transcriptional and translational levels (Figure 4C–E). Next, we used the von Frey test to measure the PWT in the innervation areas of L4 (medial plantar region) and L5 (lateral plantar region) spinal nerves, respectively.[33] We found that the PWT was elevated in the L4-innervated area but not L5 in the TAK-242 injection group (Figure 4F). Additionally, we did not observe any significant difference in thermal sensitivity between the treatment group and the non-treatment group (Figure 4G). Gait analysis of the rats injected with TAK-242 presented an increase in the contact area and intensity of the right hind paw compared to the left (Figure 4H and I). Taken together, our results proved that TLR4 played a vital role in CCL2 upregulation in adjacent DRG, and the interruption of the TLR4 signal can partly relieve the pain burden of L5 compression in rats.

Activation of TLR4 Induced CCL2 Expression in vitro

To prove the function of TLR4 in sensory neuron cells, we extracted primary DRG neurons from rat L4, L5, and L6 DRGs, which consist of sciatic nerve,[13] and verified their purity by using immunofluorescence (Figure 5A). qPCR and ELISA experiments showed that administration of LPS, which is a classical TLR4 agonist, significantly upregulated the mRNA level of *Ccl2* in DRG neurons and the protein level of CCL2 in supernatant (Figure 5B). Then, we cut off the sciatic nerve after compression of the L5 spinal nerve for 3 days and put it into primary DRG neurons 24h with or

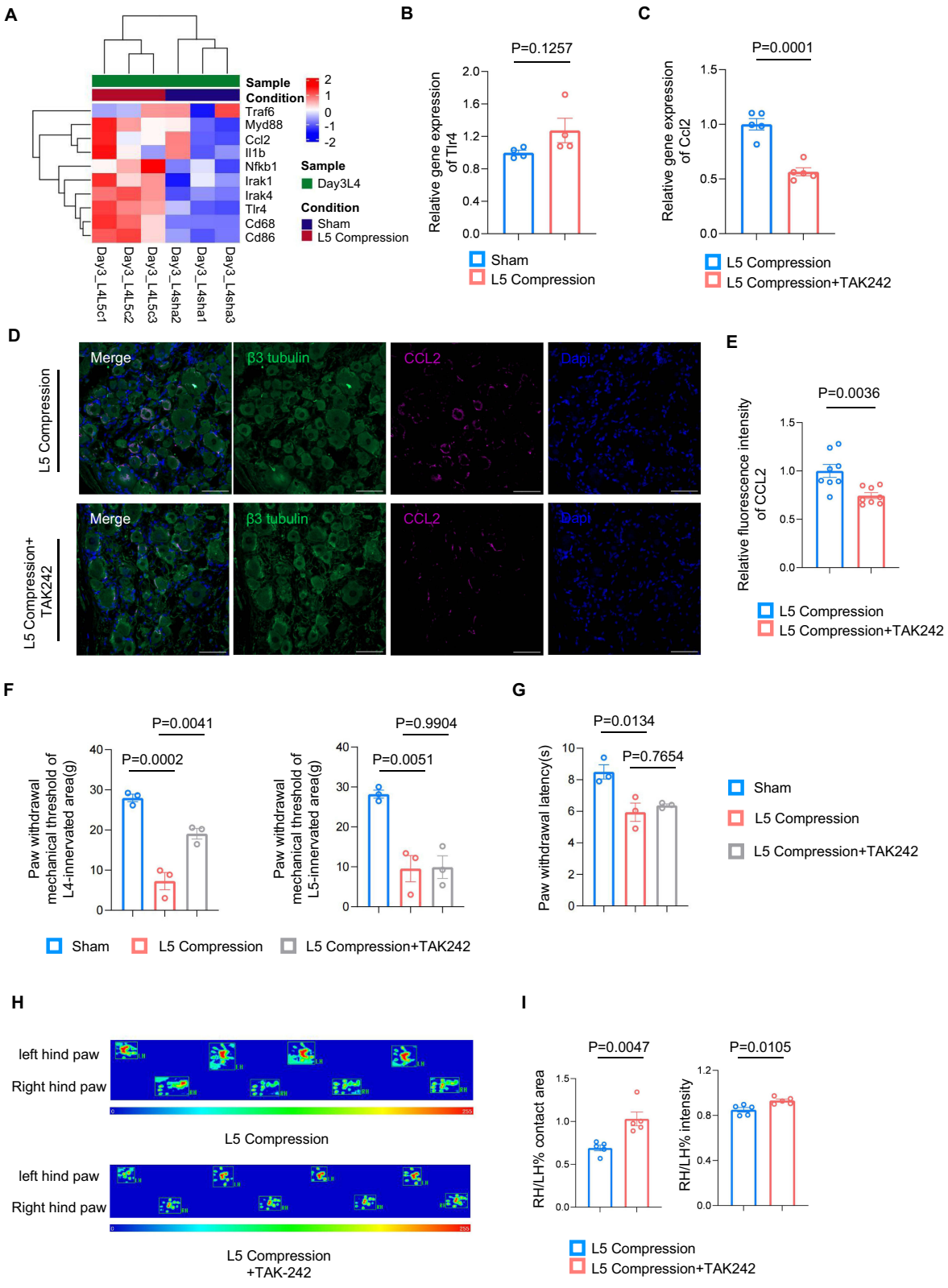

Figure 4 TAK-242 injection reduced CCL2 expression in L4 DRG. (**A**) Gene heatmap of TLR4 and CCL2 related pathway. (**B**) Relative gene expression of *Tlr4* increased (n=4). (**C**) I.p. injection with TAK-242 decreased the mRNA level of *Ccl2* on POD3 (n=5). (**D**) Representative image of CCL2 expression in rat L4 DRG on POD3. Scale bar, 50um. (**E**) Relative fluorescence intensity of CCL2 of L5 compression group versus TAK242 injection group (8 dots from 4 rats in each group). (**F**) PWT increased in L4-innervated area but not L5 after i.p. injection with TAK-242 (n=3). (**G**) PWL showed no difference after treated with TAK-242 (n=3). (**H**) Representative image of gait analysis of L5 spinal nerve compression group versus TAK-242 injection group. (**I**) I.p. injection with TAK-242 increased rat RH/LH% contact area and intensity (n=5).

https://doi.org/10.2147/JPR.S499997

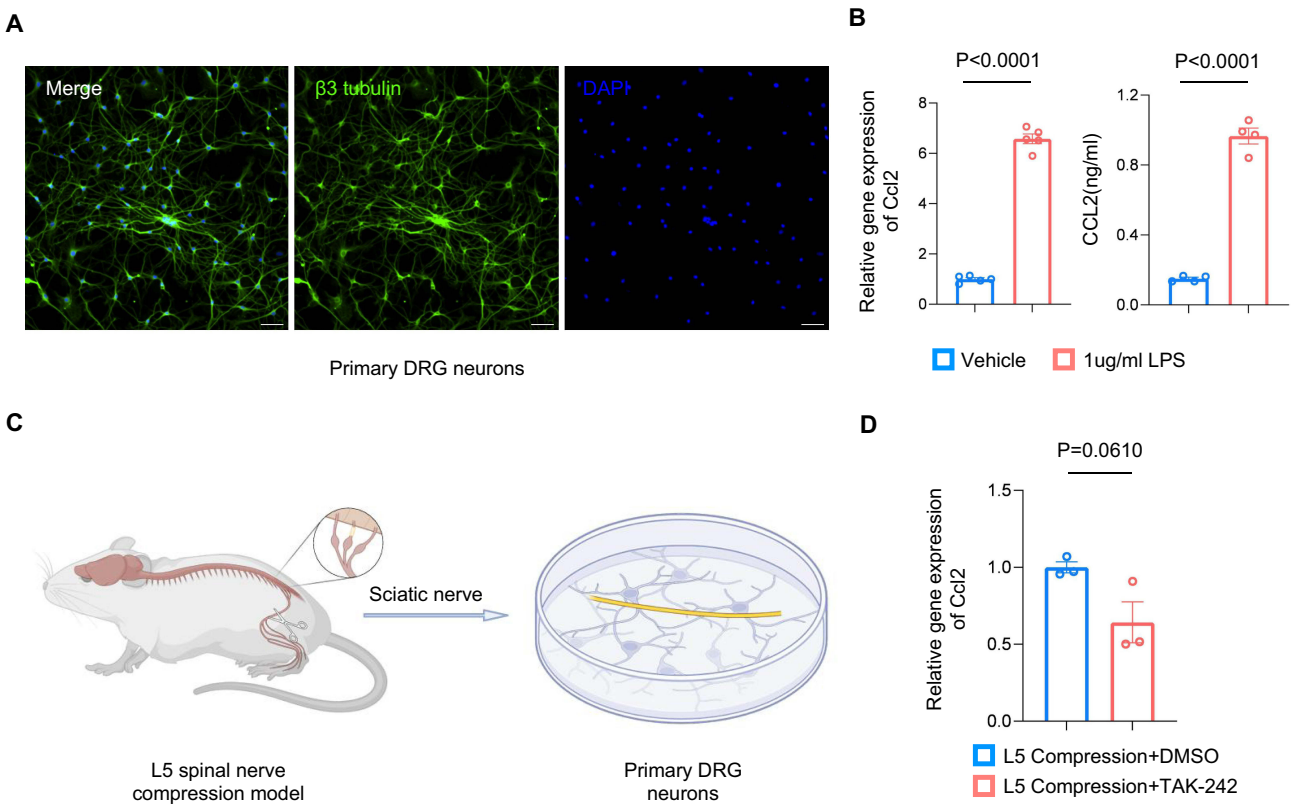

Figure 5 Activation of TLR4 induced CCL2 expression in vitro. (**A**) Representative image of rat primary DRG neurons. Scale bar, 50um. (**B**) CCL2 expression increased after stimulation with 1ug/mL LPS in DRG neurons (n=5). (**C**) Diagram of primary DRG neurons co-culture with isolated sciatic nerve from L5 compression rats. (**D**) *Ccl2* mRNA level reduced after administration of TAK-242 in the co-culture system (n=3).

without 1uM TAK-242 for 24h (Figure 5C). After washing 3 times with PBS to remove suspension cells and sciatic nerve, we evaluated *Ccl2* gene expression in adherent DRG cells. The qPCR results showed that *Ccl2* expression had a reduced trend towards significance in DRG neurons after administration of TAK-242 (Figure 5D). Above all, these results indicated that activation of TLR4 can promote CCL2 generation in isolated sensory neurons.

Discussion

In this study, we established an L5 spinal nerve compression model to investigate the mechanism of abnormal activation of the adjacent intact nerve segment. Our results showed that CCL2 was upregulated in L4 DRG after L5 nerve compression. Since L4 and L5 fibers comingle in the sciatic nerve in rats, DAMPs generated by L5 axonal degeneration activate TLR4 in L4 neurons, inducing CCL2 expression. Administration of TLR4 antagonist, TAK-242, reduced the level of CCL2 in L4 neurons and attenuated pain-like behavior after L5 nerve compression. Together, these studies indicated that activation of the TLR4/CCL2 pathway played a crucial role in radicular injury-induced global nerve trunk hypersensitivity.

Many nerve injury models were used to investigate the development of neuropathic pain, including partial sciatic nerve ligation (PSNL), chronic constriction injury (CCI), spared nerve injury (SNI), and spinal nerve ligation (SNL).[34] Different models produce different pathological changes; hence, it is crucial to establish a model to mimic specific diseases. The most common reasons for painful radiculopathy are lumbar disc herniation and intervertebral foramen stenosis.[3] However, a kind of spinal nerve compression model is absent. In our research, a 0.5mm-diameter cannula was utilized to wrap the right L5 spinal nerve, with the minimum damage to L4 axons, as LFB staining showed. After surgery, the von Frey test revealed a decreased PWT in the L5 nerve compression group. Gait analysis showed reduced right hind paw contact area and intensity, especially in the center of the plantar area, which is innervated by both L4 and L5 spinal

nerves.[35] Our L5 nerve compression model did not lead to complete limb disability or autotomy, suggesting the potential application of this model in exploring painful radiculopathy-related work.

Injured nerves were reported to be sensitized and carry amplified signals to the central nervous system, causing hyperalgesia.[2,36] However, previous studies have shown that the receptive field area was increased in L4 nerves after L5 SNL.[37] Meanwhile, an L5 dorsal rhizotomy before or after L5 SNL only partly reversed pain-like behavior while loss of L4 nociceptors in rats abolished L5 SNL-produced mechanical hypersensitivity.[7,12] Furthermore, even though only efferent neurons were damaged, paresthesia and neuropathic pain were still generated by neighboring sensory neurons.[5,10] These results suggested that adjacent intact nerve segments might also play an indispensable role in neuropathic pain.[5–7,9–12,38,39] Some research indicates that L4 neurons were activated after L5 nerve injury. L5 spinal nerve axotomy led to the spontaneous firing and lower electrical threshold in both L4 nociceptors and Aα/β-low threshold mechanoreceptors.[7,9,10] Furthermore, action potential (AP) height is significantly increased in L4 Aδ fibers, and AP overshoot is elevated in Aβ fibers.[38] The underlying mechanisms of abnormal activation of L4 fibers were proposed. Injury of the L5 spinal nerve produced a population consisting of degenerated L5 fibers and intact L4 fibers in the sciatic nerve. Dedifferentiated Schwann cells and infiltrated leukocytes secreted abundant inflammatory and neurotrophic factors.[10] Activation or upregulation of kinases and ion channels by these factors mediated hypersensitivity. For instance, after L5 spinal nerve cutting, HMGB1, a DAMP, derived from macrophages accumulating in the sciatic nerve triggers upregulation of early growth response 1 (Egr-1) and delayed increase of ubiquitin-specific protease 5 (USP5) through activation of advanced glycation end-products (RAGE), resulting in increased expression of Cav3.2 and contributing to the development of neuropathic pain.[11] Additionally, nerve growth factor (NGF) is increased in the degeneration environment and transported to L4 DRG, leading to the activation of p38 mitogen-activated protein kinase (MAPK) and upregulation of BDNF and TRPV1.[6] Consistently, local application of capsaicin to the ipsilateral sciatic or L4 spinal nerve and loss of capsaicin-sensitive L4 afferent neurons both abolished L5 SNL-produced mechanical hypersensitivity.[12] Above all, after injury, the axonal degeneration could change the properties of uninjured neurons in the same nerve trunk, the underlying mechanisms deserve our exploration.

In our study, elevated expression of CCL2 was observed in L4 DRG on both POD3 and POD7. CCL2 is a small secreted protein that functions as an important proinflammatory mediator and plays a pivotal role in the peripheral mechanisms of neuropathic pain.[14,28] Intrathecal injection of CCL2 produces rapid hypersensitivity, and administration of CCL2-neutralizing antibodies or CCR2 antagonists alleviates mechanical allodynia.[14] On the one hand, CCL2 can recruit inflammatory cells, such as monocytes. Expanded monocytes participate in the development of neuroinflammation and neuropathic pain. Our results showed that $CD68^+$ cells increased in L4 DRG after L5 nerve compression. However, it is worth pointing out that, in contrast to previous findings,[18] novel research indicated that macrophage expansion was mainly derived from local proliferation but not peripheral blood monocyte infiltration.[40] On the other hand, CCL2 depolarized the membrane potential and reduced the threshold of action potential in dissociated ganglia.[41] DRG neurons express CC chemokine receptor 2 (CCR2), which can bind with CCL2, upregulating or sensitizing ion channels.[16,41] Consistently, we found that the expression of sodium ion channels and TRPV1 increased on POD7, although we cannot rule out the effect of other inflammatory factors. In summary, after L5 nerve compression, CCL2 upregulation may serve as an endogenous initiator for the abnormal sensitization of L4 neurons.

DAMPs are alarm signals generated by distressed or injured cells and can be divided into nucleic acids, proteins, ions, glycans, and metabolites.[42] These endogenous molecules are recognized or sensed by DAMP-sensing receptors, which are widely expressed in both immune and non-immune cells. TLR4 is a classical toll-like receptor sensing multiple kinds of DAMPs, including high mobility group box 1 (HMGB1), s100s, cold-inducible RNA-binding protein (CIRP), and tenascin C.[42] In the process of nerve injury and neurodegenerative diseases, DAMPs generated in an inflammatory environment can activate TLR4 signaling in neurons.[19,43] Furthermore, in osteoarthritis patients, DAMPs were elevated in synovium or synovial fluid and proven to stimulate CCL2 expression in nociceptive neurons through TLR4,[44] resulting in mechanical hypersensitivity.[31,32] Our research showed that after L5 spinal nerve compression, the generation of CCL2 in L4 DRG neurons depended on TLR4 activation. RNA-seq of the sciatic nerve indicated an increase of DAMPs, which may serve as TLR4 agonists. Additionally, TLR4 was mainly expressed by small to medium-diameter neurons,[31] consistent with our finding that CCL2 elevation occurred in the same size neurons.

Some limitations in our studies must be considered. Firstly, in painful radiculopathy, spinal nerve compression can occur either proximal or distal to the DRG,[45] however, our model only compressed the distal side. Previous studies have predominantly damaged spinal nerves distal to the DRG.[34] This may stem from the fact that inducing proximal nerve injury requires laminectomy, which causes more extensive surgical trauma. Future research may develop refined surgery to simulate the compression of the proximal side. Secondly, the downstream pathways of TLR4 activation-induced CCL2 expression were not elucidated. TLR4-Myd88-NfkB is a well-known signaling pathway in cytokine production,[19] however, we only showed related gene upregulation in the heatmap, and whether this pathway is responsible for CCL2 elevation in L4 neurons after L5 compression needs further exploration. Additionally, Notch signaling activation and CCL2 increases were observed in LPS-stimulated DRG cell cultures,[32] which may also serve as a downstream pathway. Thirdly, although TLR4 antagonist, TAK-242, has been studied in large randomized trials for the treatment of sepsis with outcomes that demonstrate acceptable safety and tolerability profiles,[46] clinical data for treating pain is limited, and it needs further pre-clinical experiments. Finally, men and women differentially develop chronic pain conditions.[47] After nerve injury, TLR4-deficient males showed reduced allodynia, while this seems to be TLR4-independent in female mice.[48] Meanwhile, intrathecally administration of a TLR4 agonist only induced hypersensitivity in male mice.[49] These works indicate the need for carefully controlled studies examining the role of TLR4 and sex differences in persistent pain states.

Overall, our study highlights the potential therapeutic value of inhibiting the TLR4 signal in DRG neurons for the treatment of painful radiculopathy. After L5 spinal nerve compression, inflammatory cells, activated Schwann cells, and degenerative neurons generate various DAMPs, further stimulating intact L4 fibers in the sciatic nerve trunk through TLR4, inducing CCL2 production. Blockage of TLR4 with TAK-242 significantly relieves pain-like behavior and partially reduces CCL2 expression in L4 DRG. Further investigations are required to better understand the mechanisms, safety, and effectiveness of TLR4 antagonists. Nevertheless, our findings offer a novel insight into radicular injury-induced global nerve trunk hypersensitivity.

Conclusions

In conclusion, our study suggests that DAMPs derived from injured nerves trigger TLR4-dependent CCL2 overexpression in adjacent uninjured neurons in a rat model of painful radiculopathy. Administration of TLR4 antagonist, TAK-242, partly elevates paw withdrawal threshold and decreases the expression of CCL2. Thus, DAMPs, TLR4, and CCL2 could be therapeutic targets for the treatment of neuropathic pain.

Data Sharing Statement

RNA sequencing data have been deposited into GEO repository under accession codes GSE246156. Data will be made available on request.

Ethic Approval

All animal experiments were approved by the Animal Care and Use Committee of Shanghai Sixth People's Hospital (Approval No. DWLL2024-0657) according to the guidelines of the Chinese Laboratory Animal Welfare Law (GB/T 35892-2018).

Author Contributions

All authors made a significant contribution to the work reported, whether that is in the conception, study design, execution, acquisition of data, analysis and interpretation, or in all these areas; took part in drafting, revising or critically reviewing the article; gave final approval of the version to be published; have agreed on the journal to which the article has been submitted; and agree to be accountable for all aspects of the work.

Funding

This work was supported in part by the National Natural Science Foundation of China (82072525 to Y.G.H).

Disclosure

The authors declare no competing interests in this work.

References

1. Scholz J, Finnerup NB, Attal N, et al. The IASP classification of chronic pain for ICD-11: chronic neuropathic pain. *Pain*. 2019;160:53–59. doi:10.1097/j.pain.0000000000001365
2. Ghazisaeidi S, Muley MM, Salter MW. Neuropathic pain: mechanisms, sex differences, and potential therapies for a global problem. *Annu Rev Pharmacol Toxicol*. 2023;63:565–583. doi:10.1146/annurev-pharmtox-051421-112259
3. Finnerup NB, Kuner R, Jensen TS. Neuropathic pain: from mechanisms to treatment. *Physiol Rev*. 2021;101:259–301. doi:10.1152/physrev.00045.2019
4. Peene L, Cohen SP, Kallewaard JW, et al. 1. Lumbosacral radicular pain. *Pain Pract*. 2024;24:525–552. doi:10.1111/papr.13317
5. Richardson JK, Forman GM, Riley B. An electrophysiological exploration of the double crush hypothesis. *Muscle Nerve*. 1999;22:71–77. doi:10.1002/(sici)1097-4598(199901)22:1<71::aid-mus11>3.0.co;2-s
6. Obata K, Yamanaka H, Kobayashi K, et al. Role of mitogen-activated protein kinase activation in injured and intact primary afferent neurons for mechanical and heat hypersensitivity after spinal nerve ligation. *J Neurosci*. 2004;24:10211–10222. doi:10.1523/JNEUROSCI.3388-04.2004
7. Wu G, Ringkamp M, Hartke TV, et al. Early onset of spontaneous activity in uninjured C-fiber nociceptors after injury to neighboring nerve fibers. *J Neurosci*. 2001;21:RC140. doi:10.1523/JNEUROSCI.21-08-j0002.2001
8. Yu G, Segel I, Zhang Z, et al. Dorsal root ganglion stimulation alleviates pain-related behaviors in rats with nerve injury and osteoarthritis. *Anesthesiology*. 2020;133:408–425. doi:10.1097/ALN.0000000000003348
9. Djouhri L, Fang X, Koutsikou S, et al. Partial nerve injury induces electrophysiological changes in conducting (uninjured) nociceptive and nonnociceptive DRG neurons: possible relationships to aspects of peripheral neuropathic pain and paresthesias. *Pain*. 2012;153:1824–1836. doi:10.1016/j.pain.2012.04.019
10. Wu G, Ringkamp M, Murinson BB, et al. Degeneration of myelinated efferent fibers induces spontaneous activity in uninjured C-fiber afferents. *J Neurosci*. 2002;22:7746–7753. doi:10.1523/JNEUROSCI.22-17-07746.2002
11. Tomita S, Sekiguchi F, Kasanami Y, et al. Ca(v)3.2 overexpression in L4 dorsal root ganglion neurons after L5 spinal nerve cutting involves Egr-1, USP5 and HMGB1 in rats: an emerging signaling pathway for neuropathic pain. *Eur J Pharmacol*. 2020;888:173587. doi:10.1016/j.ejphar.2020.173587
12. Jang JH, Kim KH, Nam TS, et al. The role of uninjured C-afferents and injured afferents in the generation of mechanical hypersensitivity after partial peripheral nerve injury in the rat. *Exp Neurol*. 2007;204:288–298. doi:10.1016/j.expneurol.2006.11.004
13. Rigaud M, Gemes G, Barabas ME, et al. Species and strain differences in rodent sciatic nerve anatomy: implications for studies of neuropathic pain. *Pain*. 2008;136:188–201. doi:10.1016/j.pain.2008.01.016
14. Du S, Wu S, Feng X, et al. A nerve injury-specific long noncoding RNA promotes neuropathic pain by increasing Ccl2 expression. *J Clin Invest*. 2022;132. doi:10.1172/JCI153563
15. Illias AM, Gist AC, Zhang H, et al. Chemokine CCL2 and its receptor CCR2 in the dorsal root ganglion contribute to oxaliplatin-induced mechanical hypersensitivity. *Pain*. 2018;159:1308–1316. doi:10.1097/j.pain.0000000000001212
16. Jung H, Toth PT, White FA, et al. Monocyte chemoattractant protein-1 functions as a neuromodulator in dorsal root ganglia neurons. *J Neurochem*. 2008;104:254–263. doi:10.1111/j.1471-4159.2007.04969.x
17. Van Steenwinckel J, Auvynet C, Sapienza A, et al. Stromal cell-derived CCL2 drives neuropathic pain states through myeloid cell infiltration in injured nerve. *Brain Behav Immun*. 2015;45:198–210. doi:10.1016/j.bbi.2014.10.016
18. Bravo-Caparros I, Ruiz-Cantero MC, Perazzoli G, et al. Sigma-1 receptors control neuropathic pain and macrophage infiltration into the dorsal root ganglion after peripheral nerve injury. *FASEB J*. 2020;34:5951–5966. doi:10.1096/fj.201901921R
19. Acioglu C, Heary RF, Elkabes S. Roles of neuronal toll-like receptors in neuropathic pain and central nervous system injuries and diseases. *Brain Behav Immun*. 2022;102:163–178. doi:10.1016/j.bbi.2022.02.016
20. Chen Y, Dong Y, Zhang ZL, et al. Fra-1 induces apoptosis and neuroinflammation by targeting S100A8 to modulate TLR4 pathways in spinal cord ischemia/reperfusion injury. *Brain Pathol*. 2023;33:e13113. doi:10.1111/bpa.13113
21. Dobin A, Davis CA, Schlesinger F, et al. STAR: ultrafast universal RNA-seq aligner. *Bioinformatics*. 2013;29:15–21. doi:10.1093/bioinformatics/bts635
22. Liao Y, Smyth GK, Shi W. featureCounts: an efficient general purpose program for assigning sequence reads to genomic features. *Bioinformatics*. 2014;30:923–930. doi:10.1093/bioinformatics/btt656
23. Love MI, Huber W, Anders S. Moderated estimation of fold change and dispersion for RNA-seq data with DESeq2. *Genome Biol*. 2014;15:550. doi:10.1186/s13059-014-0550-8
24. Yu G, Wang LG, Han Y, et al. clusterProfiler: an R package for comparing biological themes among gene clusters. *OMICS*. 2012;16:284–287. doi:10.1089/omi.2011.0118
25. Subramanian A, Tamayo P, Mootha VK, et al. Gene set enrichment analysis: a knowledge-based approach for interpreting genome-wide expression profiles. *Proc Natl Acad Sci U S A*. 2005;102:15545–15550. doi:10.1073/pnas.0506580102
26. Lei M, Wang W, Zhang H, et al. Cell-cell and cell-matrix adhesion regulated by Piezo1 is critical for stiffness-dependent DRG neuron aggregation. *Cell Rep*. 2023;42:113522. doi:10.1016/j.celrep.2023.113522
27. Beckworth WJ, Abramoff BA, Bailey IM, et al. Acute cervical radiculopathy outcomes: soft disc herniations vs osteophytes. *Pain Med*. 2021;22:561–566. doi:10.1093/pm/pnaa341
28. Jiang BC, Liu T, Gao YJ. Chemokines in chronic pain: cellular and molecular mechanisms and therapeutic potential. *Pharmacol Ther*. 2020;212:107581. doi:10.1016/j.pharmthera.2020.107581
29. Schappacher KA, Xie W, Zhang JM, et al. Neonatal vincristine administration modulates intrinsic neuronal excitability in the rat dorsal root ganglion and spinal dorsal horn during adolescence. *Pain*. 2019;160:645–657. doi:10.1097/j.pain.0000000000001444

30. Geisler S, Doan RA, Strickland A, et al. Prevention of vincristine-induced peripheral neuropathy by genetic deletion of SARM1 in mice. *Brain*. 2016;139:3092–3108. doi:10.1093/brain/aww251
31. Miller RE, Belmadani A, Ishihara S, et al. Damage-associated molecular patterns generated in osteoarthritis directly excite murine nociceptive neurons through Toll-like receptor 4. *Arthritis Rheumatol*. 2015;67:2933–2943. doi:10.1002/art.39291
32. Wang L, Ishihara S, Li J, et al. Notch signaling is activated in knee-innervating dorsal root ganglia in experimental models of osteoarthritis joint pain. *Arthritis Res Ther*. 2023;25:63. doi:10.1186/s13075-023-03039-1
33. Takahashi Y, Aoki Y, Doya H. Segmental somatotopic organization of cutaneous afferent fibers in the lumbar spinal cord dorsal horn in rats. *Anat Sci Int*. 2007;82:24–30. doi:10.1111/j.1447-073X.2006.00164.x
34. Ristoiu V. Contribution of macrophages to peripheral neuropathic pain pathogenesis. *Life Sci*. 2013;93:870–881. doi:10.1016/j.lfs.2013.10.005
35. Cobianchi S, de Cruz J, Navarro X. Assessment of sensory thresholds and nociceptive fiber growth after sciatic nerve injury reveals the differential contribution of collateral reinnervation and nerve regeneration to neuropathic pain. *Exp Neurol*. 2014;255:1–11. doi:10.1016/j.expneurol.2014.02.008
36. Yu X, Liu H, Hamel KA, et al. Dorsal root ganglion macrophages contribute to both the initiation and persistence of neuropathic pain. *Nat Commun*. 2020;11:264. doi:10.1038/s41467-019-13839-2
37. Boada MD, Gutierrez S, Aschenbrenner CA, et al. Nerve injury induces a new profile of tactile and mechanical nociceptor input from undamaged peripheral afferents. *J Neurophysiol*. 2015;113:100–109. doi:10.1152/jn.00506.2014
38. Djouhri L, Zeidan A, Alzoghaibi M, et al. L5 spinal nerve axotomy induces distinct electrophysiological changes in axotomized L5- and adjacent L4-dorsal root ganglion neurons in rats in vivo. *J Neurotrauma*. 2021;38:330–341. doi:10.1089/neu.2020.7264
39. Kim HW, Shim SW, Zhao AM, et al. Long-term tactile hypersensitivity after nerve crush injury in mice is characterized by the persistence of intact sensory axons. *Pain*. 2023;164:2327–2342. doi:10.1097/j.pain.0000000000002937
40. Guimaraes RM, Anibal-Silva CE, Davoli-Ferreira M, et al. Neuron-associated macrophage proliferation in the sensory ganglia is associated with peripheral nerve injury-induced neuropathic pain involving CX3CR1 signaling. *Elife*. 2023;12:e78515. doi:10.7554/eLife.78515
41. Sun JH, Yang B, Donnelly DF, et al. MCP-1 enhances excitability of nociceptive neurons in chronically compressed dorsal root ganglia. *J Neurophysiol*. 2006;96:2189–2199. doi:10.1152/jn.00222.2006
42. Ma M, Jiang W, Zhou R. DAMPs and DAMP-sensing receptors in inflammation and diseases. *Immunity*. 2024;57:752–771. doi:10.1016/j.immuni.2024.03.002
43. Kobayashi D, Kiguchi N, Saika F, et al. Insufficient efferocytosis by M2-like macrophages as a possible mechanism of neuropathic pain induced by nerve injury. *Biochem Biophys Res Commun*. 2020. doi:10.1016/j.bbrc.2020.02.032
44. Sohn DH, Sokolove J, Sharpe O, et al. Plasma proteins present in osteoarthritic synovial fluid can stimulate cytokine production via toll-like receptor 4. *Arthritis Res Ther*. 2012;14:R7. doi:10.1186/ar3555
45. Berry JA, Elia C, Saini HS, et al. A review of lumbar radiculopathy, diagnosis, and treatment. *Cureus*. 2019;11:e5934. doi:10.7759/cureus.5934
46. Rice TW, Wheeler AP, Bernard GR, et al. A randomized, double-blind, placebo-controlled trial of TAK-242 for the treatment of severe sepsis. *Crit Care Med*. 2010;38:1685–1694. doi:10.1097/CCM.0b013e3181e7c5c9
47. Bruno K, Woller SA, Miller YI, et al. Targeting toll-like receptor-4 (TLR4)-an emerging therapeutic target for persistent pain states. *Pain*. 2018;159:1908–1915. doi:10.1097/j.pain.0000000000001306
48. Stokes JA, Cheung J, Eddinger K, et al. Toll-like receptor signaling adapter proteins govern spread of neuropathic pain and recovery following nerve injury in male mice. *J Neuroinflammation*. 2013;10:148. doi:10.1186/1742-2094-10-148
49. Sorge RE, LaCroix-Fralish ML, Tuttle AH, et al. Spinal cord toll-like receptor 4 mediates inflammatory and neuropathic hypersensitivity in male but not female mice. *J Neurosci*. 2011;31:15450–15454. doi:10.1523/JNEUROSCI.3859-11.2011